Unstable behavior of pump-turbines and its effects on power regulation capacity of pumped-hydro energy storage plants

Giovanna Cavazzini[a*], Jean-Bernard Houdeline[b], Giorgio Pavesi[a], Olivier Teller[b], Guido Ardizzon[a]

[*] *corresponding author*
[a]*Department of Industrial Engineering, University of Padova, 35131 Padova, ITALY*
giovanna.cavazzini@unipd.it   guido.ardizzon@unipd.it   giorgio.pavesi@unipd.it
[b]*GE Renewable Energy, 38041 Grenoble, FRANCE*
jean-bernard.houdeline@ge.com, olivier.teller@ge.com

Intermittent renewable energy sources are characterized by a highly fluctuating, unpredictable and delocalized energy production, which significantly limits their penetration in the grid due to the great problems caused in the balance between demand and supply.

Pumped Hydro Energy Storage plants represent an ideal solution because of their ability to provide large storage capacity with excellent grid connection properties, high cycle efficiency range and competitive costs. However, to provide primary and secondary regulation services, PHES have to increase their operation at part loads and to be able to switch fast and frequently between pump and turbine modes. At these operating conditions, pump-turbines suffer from behaviour instabilities, thereby constituting a limit when considering their exploitation in a wider continuous working range. So, the definition of a new concept of pump-turbines able to provide the full benefit of regulation in pumping mode and a wide range of power in generation mode is an urgent need to increase the exploitation of renewable energy sources.

This paper clarifies the effects of the stable and unstable behaviour of pump-turbines on the power regulation capacity of pumped hydro energy storage plants, by presenting a description of the possible operating modes of PHES and by focusing on the impact of the hydraulic characteristics of pump-turbines on the capability of plant to start-up, shut-down or change its operating modes.

A detailed review of the studies published in literature on the topic revealed the main characteristics of the hydraulic instabilities and the influence of one or more geometrical parameters on their onset. Even though some geometry modifications aimed at improving the RPT's stability in one operating mode were proposed in literature, the definition of a comprehensive design strategy, globally optimizing the pump-turbine design by considering simultaneously the complexity of the phenomena in both the operating modes, still represents a challenge.

Keywords: pump-turbine, hump zone, S-Shape, unstable behavior, pumped-hydro, storage

1. Introduction

There has been a significant increase in the production of green energy from renewable energy sources, even if the deployment of their huge potential is still limited by the negative impact of the unpredictable and

intermittent characteristics of these sources on the safety, stability and efficiency of the electricity grid, requiring the electricity supply to constantly meet the electricity demand [1]. To overcome these limits, which hamper the achievement of a carbon free electricity generation target, the grid needs to be operated in a smart way [2] and to include a higher energy storage capacity [3]–[5].

It is clear that Pumped Hydro Energy Storage plants (PHES) constitute the most cost-effective technology for boosting power regulation capabilities for plant operators, with competitive costs (300-400 €/kW) and a cycle efficiency range of 65-80% [6], [7]. Within this context, more than 7400 MW of new PHESs, generally equipped with reversible pump-turbines (RPTs), have been launched in recent years with costs totalling over 6 billion €[8]. To enhance the grid regulation capability of PHES [9], some of these plants (Linthal-Limmern, Nant de Drance, Tehri) have been equipped with the breakthrough variable-speed RPT machines, using the Doubly Fed Induction Motor generator technology (DFIM) [10], which improves the RPT efficiency over a wider operating range[11], [12]. However, even though varying the rotational speed can significantly increase the RPT operating range, repeated and faster changes between pumping and generating modes are requested together with more operation of the machine under off-design conditions [13]. In such a demanding context, the regulation capacity of PHES is still limited by some hydraulic instability developing in both pumping and generating modes. So, the definition of a new concept of pump-turbines able to provide the full benefit of regulation in pumping mode and a wider range of power in generation mode is an urgent need to increase the exploitation of renewable energy sources (not only hydropower but also intermittent sources as solar and wind). However, the key starting point for the definition of a new design strategy for pump-turbines is an in-depth understanding of the instability phenomena, limiting at the present time generation potential and frequency regulation services of PHES.

A description of the new generation of PHES with technical details on mechanical aspects of hydraulic machinery, power electronics devices and utilities operation strategies have been presented in [14] and was mainly addressed to PHES experts. The aim of this paper is to approach the topic from a more hands-on viewpoint, and to understand better the consequences of the development of instability behaviours of RPTs on the power regulation capacity of pumped hydro energy storage plants and the challenges to face in defining a new concept of pump-turbines. Therefore, the paper is set out according to the following sections: Section 2 presents a description of the possible operating modes encountered by a RPT in a PHES plant, highlighting the effects of its hydraulic characteristics on the capability of plant to start-up, shut-down or change its operating modes in order to provide regulation capability. Sections 3 and 4 present a detailed review of the studies published in literature on the unsteady phenomena developing in pumping and in generating mode respectively with a particular focus on the most significant results achieved, on the experimental and numerical approaches adopted and on the remaining challenges in designing future generations of RPT machines.

2. Stable and unstable operating modes of reversible pump-turbines

Possible gains in the regulation capability of a RPT can be achieved by increasing its capability of starting-up, shutting down and/or switching between from one mode to the other (pump to turbine and vice-versa) in the fastest way. However, since this dynamic behaviour brings the machine out of its stable and standard working range, it is necessary to examine how this enlarged working range impacts on the relevant hydraulic and mechanical quantities [15]–[17].

Due to the reversibility of shaft rotation and discharge direction, RPTs have a large operation area. The "four-quadrant diagram" provides a 360° representation of the RPT characteristic behavior. This reports all the possible operating conditions of a RTP in terms of flow rate, head, torque, rotation rate and wicket-gate openings [18]. The relationship between these performance parameters is generally expressed in terms of the evolution of the discharge factor $Q_{11} = Q \left(\frac{D_{11}}{D}\right)^2 \sqrt{\frac{H_{11}}{H}}$ [m³/s] versus the speed factor $n_{11} = n \frac{D}{D_{11}} \sqrt{\frac{H_{11}}{H}}$ [rpm], where H, Q and D are respectively head [m], flow rate [m³/s] and runner diameter [m] [19]. Such similarity factors compare the performance Q and H of a RTP at speed n with those of a geometrically similar RTP model having a diameter (D_{11}) and head (H_{11}) of 1 m. Figure 1 shows an example of this diagram by reporting the discharge-speed characteristics of a RPT at three constants guide vane openings [19].

The combination of the positive or negative direction of Q_{11} and n_{11} define the four quadrants, which correspond to the following operating modes [20]:

I. Pump Quadrant:

    The Pump Quadrant refers to the pumping mode of the RPT: the discharge (Q) and the rotational speed are both negative (n<0). Dotted lines represent the typical limits of the normal and continuous operating range in pumping mode. The left line represents the minimum available head whereas the right line represents the maximum available head of the power plant.

    The blue area corresponds to the normal and continuous operating range of the pump, consisting of operating points (such as Point A) located between the minimum and the maximum head levels, on the optimum efficiency curve.

    The operating point B corresponds to the net head at zero discharge. As necessary condition for the pump starting, the corresponding net head delivered by the pump must be higher than the gross head when guide vanes are closed (i.e. zero discharge). The absorbed power level at zero discharge is also a needed value when a back to back start-up must be considered.
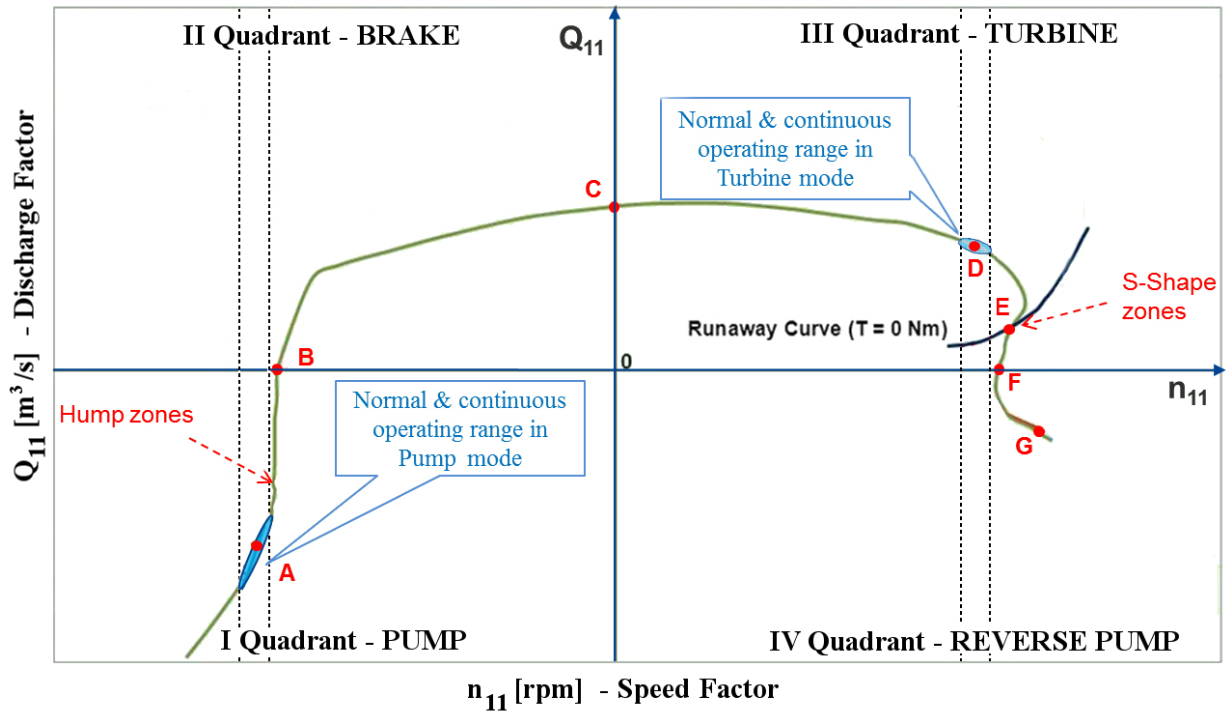
Figure 1 Typical four quadrant characteristics of a high head RPT with details of the normal operating ranges and of the unstable operating zone both in turbine and in pump mode [19]

II. Pump Brake Quadrant:

This operating mode, also called Energy Dissipation Mode, is characterized by negative rotational speed (n<0) but positive direction of discharge (Q>0).

The RTP falls in this quadrant as a consequence of a transient operation. An example can be the occurrence of a power failure in pumping mode. In this case, the failure causes a rapid reduction of RPT speed (for example from point A to point B at medium guide vane opening) combined with an inversion of the discharge direction (from negative to positive discharge) till a zero-speed discharge condition is reached (point C).

When needed, it is also useful for a fast mode change from pumping to generating mode without complete closing of the guide vanes.

III. Turbine Quadrant:

This Quadrant refers to the generating mode of the RPT and is hence characterized by positive direction of rotational speed (n>0) and discharge (Q>0).

The blue area corresponds to the normal and continuous operating range of the RPT in this mode, in which point D represents one of the numerous operating points. This operating area, corresponding also to the optimum efficiency area of this quadrant, is limited on one side by the maximum available head (minimum speed factor – left dotted line) and one the other by the minimum available head (maximum speed factor – right dotted line). This operating area is also limited by the full load output level (corresponding to the maximum discharge level) and by a partial load output level (corresponding to the

minimum discharge level). The usual partial load limit of power output (and for a given head) is set around 50% of full load output.

The operating point C corresponds to zero-speed discharge and break-away torque while the operating point E corresponds to turbine runaway, a particular operating condition of zero torque and hence of no-load on the RPT shaft. The runaway curve reported in Figure 1 identifies the no-load operating conditions as a function of the guide-vane opening and of the speed factor.

In this quadrant, the area between the runaway curve and x-axis identifies a specific pump-turbine mode, called "turbine brake", characterized by negative torque delivered to the machine shaft. The operating point F corresponds to the zero-discharge specific hydraulic energy in turbine mode.

Turbine and turbine brake modes are also important during transient operation in case of generator disconnection in turbine operation.

IV. Reverse Pump Quadrant:

This Quadrant refers to the Reverse pump mode and is characterized by positive direction of rotational speed (n>0) but negative direction of discharge (Q<0). It can only be reached in transient condition (Point G).

2.1 Effects of the unstable behaviour in pumping mode

The normal and continuous operating range of a reversible machine both in pumping and generation mode (blue areas in Figure 1) is mainly limited by stability problems related to the onset and development of an unstable behaviour of the machine.

In pumping mode, this unstable behaviour is characterized by a zone of negative slope of the Q_{11}- n_{11} curve (the so called "hump" zone) (dQ$_{11}$/dn$_{11}$<0) such as shown in Figure 1 and, for more detail in Figure 2a, also characterized by the corresponding positive slope (dH/dQ>0) of the head-discharge curve in the hump zone [21]. A pump-turbine, working in this hump zone, could suffer the consequences of the development of unsteady phenomena inside rotating and stationary blade passages, which dissipate the fluid energy causing a decrease in head. This unstable behaviour may also lead to self-excited pulsations propagating in the plant with the onset of possible heavy damage to the PHES structure [22]. This is the reason why a continuous operation is prohibited in this hump zone for the industrial machines.

A further problem related to existence of this hump zone in the RPT characteristics is that, if this zone is located below the highest operating head (H'_{max} in Figure 2a), it could prevent the start-up of the pump at this head with obvious consequences on the plant's regulation capacity. In this case, to avoid an accidental operating in the hump area, it is usual to cover this risk using margins such as defined in Figure 2a. The margin A is considered during the start-up, whereas the margin B is considered to define the limit of the stable operating point for the maximum head level (H_{max}). However, these margins further reduce pumping operating range and regulation capacity.
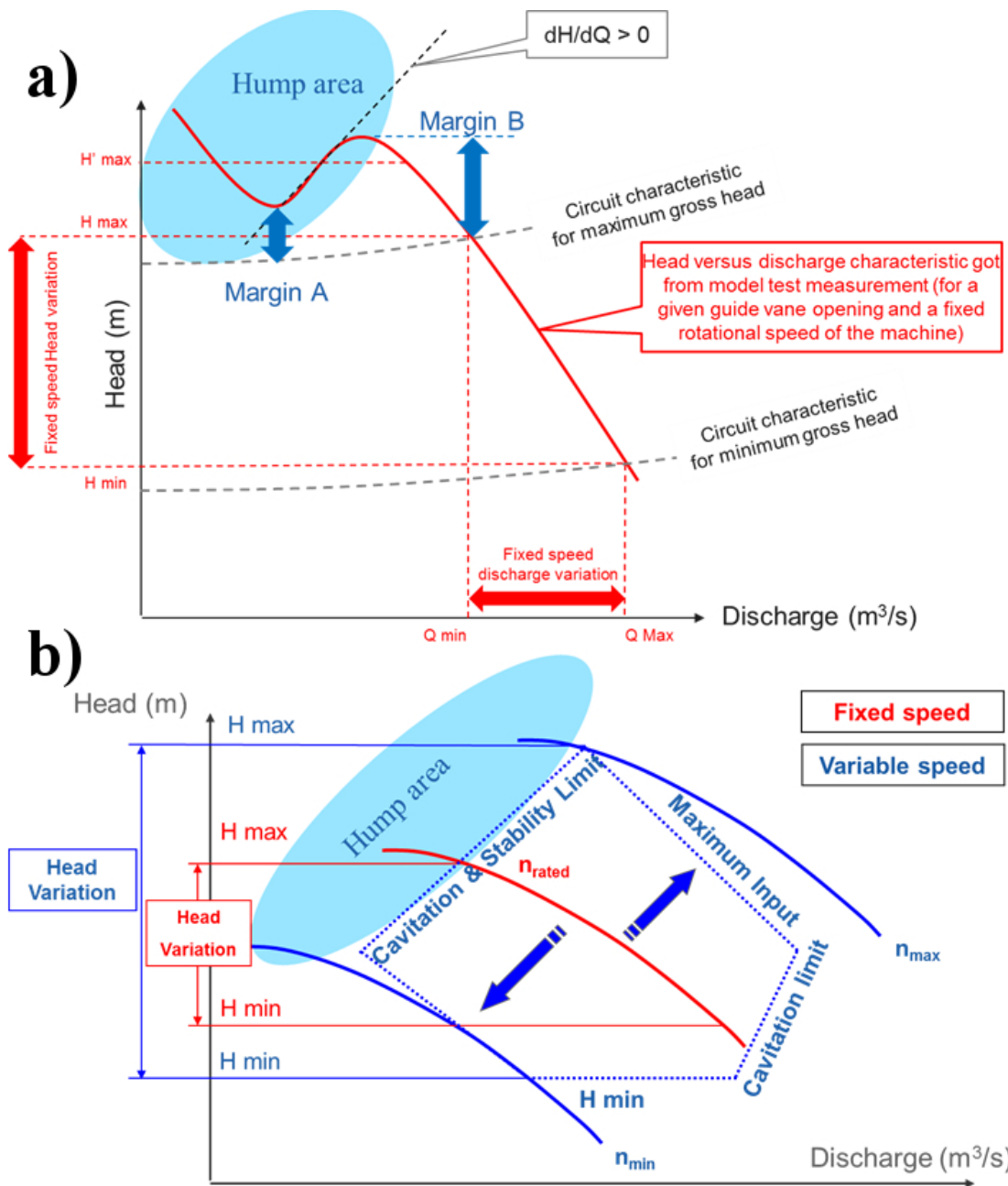
Figure 2 Comparison of operating domains between fixed (a) and variable-speed (b) pump-turbines (pumping mode)

This hump zone, which has to be excluded from the machine working range, leads to two main drawbacks:

1. It affects the industrial dimensioning of the RPT machine which directly impacts the cost of the machine as well as the power house. For a given maximum head and a rotational speed level, the sizing of machine will be even smaller if the hump zone shifts towards higher head level.

2. It significantly limits the regulation capability of the PSHP. A shift of the hump area towards highest head level increases the operating range capacity of the industrial machine. A direct benefit of this advantage is to minimize the size of the basins and thus their environmental impact.

For variable-speed RPT (Figure 2b), the RTP enlarges its working range by varying its rotation rate but, for the time being, this extension is not sufficient to solve the issue driven by the pump's hydraulic behaviour.

2.2 Effects of the unstable behaviour in generating mode

In turbine mode, an unstable behaviour of the machine begins to occur around the partial load level (usually set around 50% of full load output) and is extended up to the no-load condition. The unstable behaviour is characterized by a positive slope of the discharge-speed factors curve ($dQ_{11}/dn_{11}>0$), the so-called "S-Shaped" discharge-speed factors curve (Figure 3) and causes pronounced fluctuations and increased vibrations of the machine [23]–[25]. If this positive slope occurs at no-load conditions (red area in Figure 3), this unstable behaviour negatively affects turbine start-up and synchronization to the grid. Moreover, it also negatively affects the transient behavior of the turbine machine as well as the hydraulic circuit during turbine stopping processes, especially during emergency stops (blue area in Figure 3) [26], [27].
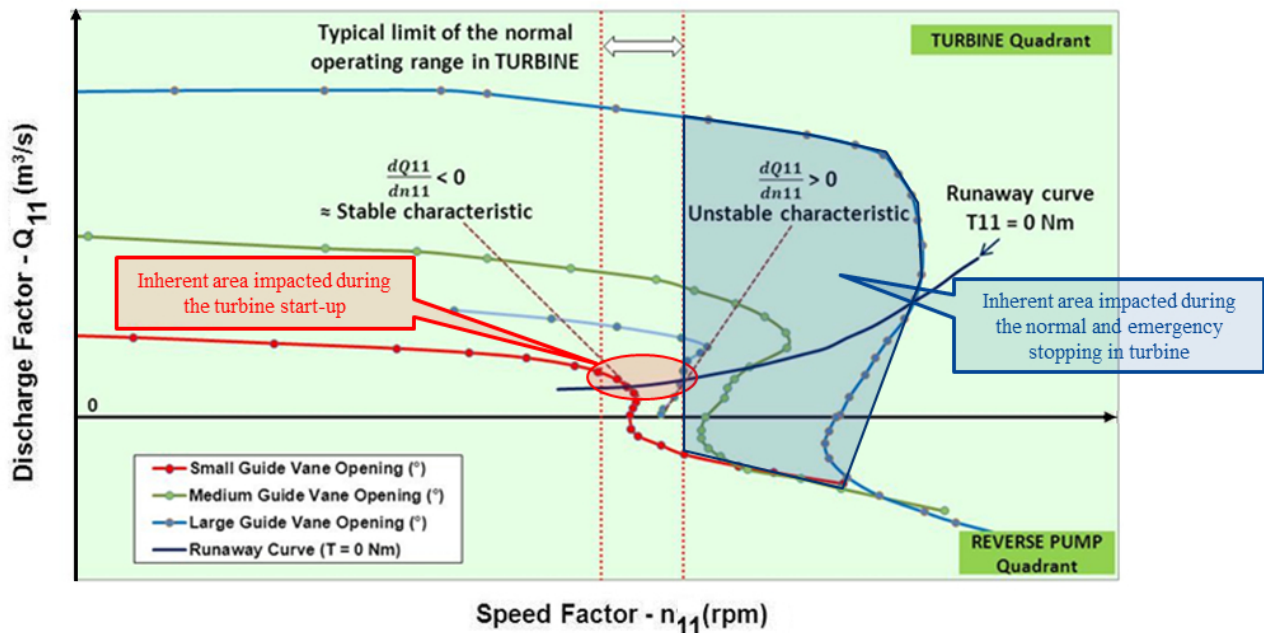

Figure 3 S-Shaped characteristic curve of a pump-turbine in turbine and reverse pump modes: discharge-speed curve for some constant guide vane openings with details of the areas impacted during turbine start-up and normal and emergency stops [19]

2.2.1 Turbine start-up and synchronization to the grid

The start-up of a RTP in generating mode requires to bring the turbine to a stable operation close to runaway curve ($T_{11}=0$). In this operating conditions, a slight opening is imposed to the synchronized guide vanes. Its frequency, proportional to the rotational speed, must be synchronized with the grid frequency and very small frequency oscillations are accepted (relatively strict coupling criteria could be below ±0.04% of the grid frequency). Since Pumped-Hydro Energy Storage Plants should guarantee high flexibility in terms of power

regulation and reaction time to deliver grid balancing services, their start-up sequence should be as fast as possible: the fastest units can start up from idle to full power in less than 90s. Turbines affected by the S Shape phenomenon at start-up cannot reach this performance and are less valuable for network operation. This is particularly true for high head units (i.e. high centrifugal pump-turbine machines) that have an S-shaped feature near the runaway curve (T_{11}=0) in turbine mode. For example, Figure 4a reports the Q_{11}-n_{11} characteristics of a high-head RPT for several guide-vane openings [19]. As it can be seen, each curve is characterized by an S-Shape operating region (dQ_{11}/dn_{11}>0) which is located closer and closer to the runaway curve for increasing guide vane openings, determining a limit in the minimum exploitable head level (H_{min}).
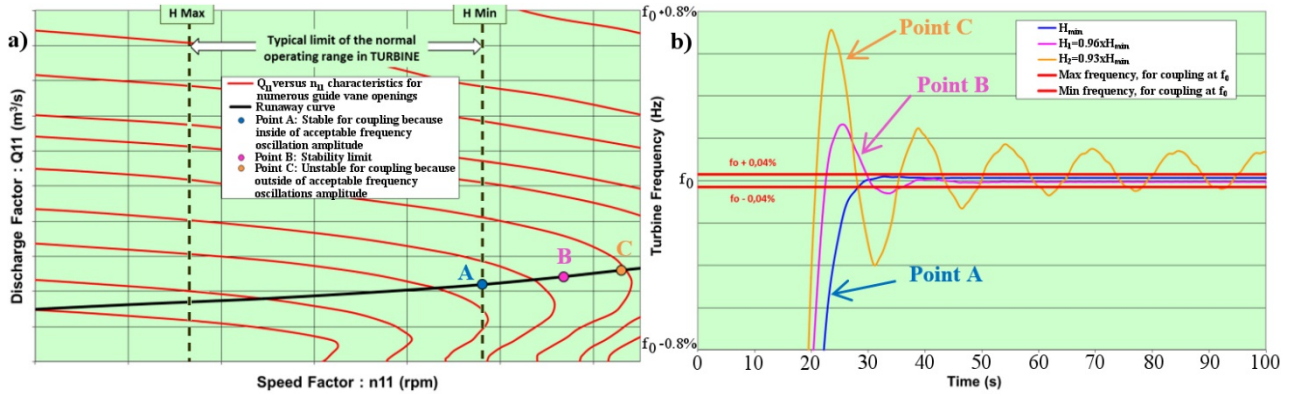

Figure 4 a) Discharge factor versus speed factor in turbine quadrant; b) Turbine frequency evolution versus time for different head levels during the start-up sequence [19]

To understand the effects of these particular Q_{11}-n_{11} characteristics on the start-up sequences, coupling sequence simulations between the high-head RPT and the grid have been carried out for three head levels, whose corresponding operating points at no-load condition have been highlighted in Figure 4a (point A in the operating range and points B and C below the minimum head level) [19]. Figure 4b reports the results of these simulations in terms of turbine frequency evolution versus time to reach the coupling condition with the grid frequency f_0.

For H_{min} (minimum gross head level) corresponding to the operation point A, the simulation results show no oscillation of the turbine rotational speed with a consequent coupling condition reached very quickly.

For the gross head H_1=0.96H_{min}, corresponding to the operation point B, during the start-up sequence some oscillations of the rotational speed due to the S-Shape region closer to the no-load condition appear. The sequence requires about 10 seconds more until oscillations of the rotational speed are damped below the acceptable value (±0.04%). However, since a stable coupling condition can be reached, the area between H_{min} and H_1=0.96H_{min} could still be used to extend the operating range if needed.

For the gross head H_2=0.93H_{min}, since the S-Shape operating region affects the no-load condition, the start-up of the pump-turbine is quite impossible due to the unstable behavior of the pump-turbine causing significant oscillation of the turbine rotational speed at this operating point C. The coupling condition is not reached because the turbine frequency oscillations versus the grid frequency are too large.

2.2.2 Transient phenomena during turbine stops

Transient phenomena occur during the starting and stopping sequences of the machine [28]. Nevertheless, the stopping sequences often lead to the most unfavourable transient behaviors for the turbine machine as well as for the hydraulic circuit, reason why they have to be studied very carefully. The different transient's scenarios can be classified according to their occurrence:

- The largest and the medium occurrence level correspond to a normal stopping and an emergency stop due to detected mechanical defaults respectively. In both cases, the circuit breaker is opened when reaching no load operation (runaway curve) at the end of the guide vanes closure.
- The lowest occurrence level corresponds to the emergency stops due to electrical defaults or grid failures (also called load rejection). In this case the circuit breaker is immediately opened and the RTP is disconnected from the grid. Due to the associate transient behaviour these emergency stops must be considered as the most critical in terms of mechanical solicitation levels, not only for the mechanical equipment of the turbine but also for the whole power plant. For a given power plant circuit, the origin of the transient behavior is mainly due to the S-Shaped characteristic curve of the turbine [29], [30].

To better understand the difference in terms of transient behaviour between a normal stop and an emergency stop caused by an electrical default (load rejection), a comparison in terms of static pressure level evolution, measured on site close to the main inlet valve (high pressure side of the machine), versus time is reported in Figure 5. Blue curve stands for the normal stop while red curve stands for the emergency stop. The rotational speed evolution of the turbine is also shown for the emergency stop while the rotational speed evolution for normal stop is not showed because remaining to a constant value (the turbine is still connected to the grid).

During a normal stop, the circuit breaker is opened, while the turbine is still connected to the grid. The rotational speed remains constant till the no-load operation is reached at the end of the guide vane closure. During this period, the static pressure close to the main inlet valve remains quite constant, testifying a quite stable behaviour of the machine. On the other side, during a load rejection scenario, the RTP disconnection from the grid causes a rapid acceleration at constant guide vane opening (red dotted line in Figure 5) and consequent important rise of the static pressure (red line in Figure 5). Near the runaway condition, for the RPT affected by the S-shape behavior each small speed variations would determine a sudden change of operating mode, forcing the RTP to continuously switch to and for from pump to turbine mode. Specific control solutions, such as adequate closing laws for the main inlet valve and/or for guide vanes, have to be put in place to avoid risks of damages to electrical and mechanical equipment of the power plant. The turbine suffers from a critical transient behaviour with a progressive reduction of the rotation speed accompanied by significant pulsations of the static pressure.

In such a context, it is clear that innovative design criteria that eliminate or, at least, move these hydraulic instabilities, which are at the origin of the S Shaped characteristic, out of the transient operating range are a key point for increasing the regulation capacity of PHES and, therefore, to benefitting and boosting electricity production from intermittent green sources.
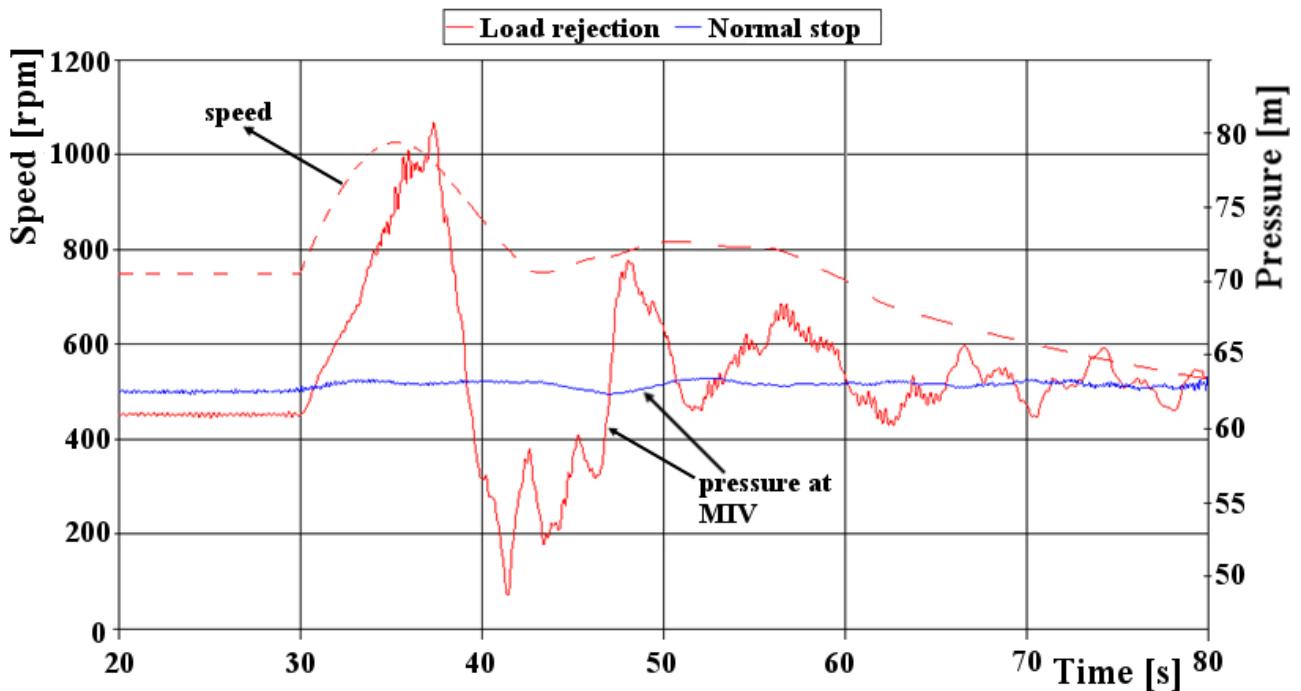
Figure 5 Comparison between emergency and normal stop behaviour: static pressure level evolution measured on site close to the main inlet valve and speed versus time [19]

3. Instability in pumping mode: the saddle zone

The saddle-type pump instability (also called "hump zone") is undoubtedly one of the biggest barriers for the enlargement of the pump normal working range (the second one being the cavitation limit on the runner's blade leading edge), even when a variable speed RPT is considered [12]. This unstable pumping operating zone is characterized by a marked interference between runner and stators (stator vanes, return channel, draft tube, adduction) with the development of flow features, such as flow separations, reverse flows and jet flows. These may cause a significant rise of the hydraulic losses with two direct negative impacts on the machine: the head drop of the RPT performance and strong pressure pulsations on the runner and guide vanes, which may lead to cracks and damages to the shear pin or to the guide vanes stem. Possible innovative design criteria aimed at eliminating or, at least, moving out of the normal and continuous operating range the hump zone, pass through the identification of the dependency between RTP's design and the onset of the unstable behavior. However, up to now, the causes of its development are under constant debate, even if possible relations with rotor/stator geometries have been argued.

Research on the connections between unsteady flows and structural vibrations can be traced back to the last century when it would focus on the wake of the runner blades, analyzing their interaction with stator blades or volute tongue. Arndt et al. [31], [32] put the radial gap between rotor and stator in relation with the intensity of pressure pulsations at the blade passage frequency (BPF). They demonstrated that a vaneless diffuser is characterized pressure fluctuations considerably smaller than those of a vaned diffuser, in which the decrease

in radial gap causes a strongly increase in flow unsteadiness. In 1992, Dong et al. [33] focused on the large fluctuations induced by the passage of the runner blade on the volute tongue and demonstrated the influence of the time-varying angular distance between runner blade and tongue tip on the pulsating characteristics of the flow field. Akin and Rockwell [34], [35] applied for the first time the High-Image-Density Particle Image Velocimetry on a pump, showing the instantaneous flow fields in the region between rotor and stator blades. A complex three-dimensional flow structure, characterized by stall cell and vortexes, resulted to develop at off-design conditions near the runner blade trailing edge and in the stator blade channel. Even in this case, the structure characteristics were strongly dependent on the time-varying angular distance between the runner blade trailing edge and the blade leading edge.

The rotor-stator interaction (RSI) area in a centrifugal pump was also investigated by Sinha et al. [36] who presented a thorough fluid-dynamical analysis using Particle Image Velocimetry (PIV) combined with unsteady pressure transducers. Their experimental analysis focused on the hump zone of the pump characteristic curve, identifying the onset of a rotating stall in the stator, negatively impacting on a number of diffuser channels, whose flow fields resulted to be alternatively characterized by outward jetting and reverse flow. A similar analysis was proposed by Sano et al. [37] who identified a "leakage" stream, moving from one stator channel to the other via the radial gap between runner and diffuser, as the cause of the onset of a rotating movement in initially stationary stall cells. Both the studies [36], [37] identified the radial gap as a geometrical factor affecting the onset of flow instabilities in stator parts (diffuser and/or volute). In particular, they demonstrated that larger radial gaps increase the probability of the stall onset and amplify its influence on the stator flow fields, whereas narrower gaps reduce the intensity of the leakage flow, determining a more intense circumferential pressure gradient and leakage flow into the volute.

Gonzalez et al. [38] for the first time numerically and experimentally analyzed the mutual fluid-dynamical influence of the runner on the volute and vice versa. They demonstrated that the interaction between the three-dimensional flow field coming out from the runner passages and the volute tongue caused the onset of pressure pulsations in the radial gap near the runner exit, having a frequency equal to that of the runner blade passage. The intensity of the pressure fluctuations increased at part loads because of the off-design incidence condition on the volute tongue, increasing the energy losses and limiting the operating range of the machine. Moreover, they demonstrated that the numerical analysis can replicate this rotor-stator interaction (RSI) phenomenon both in terms of flow and pressure fluctuations. They also highlighted that this type of RSI numerical analysis required to fix total absolute pressure and static pressure as boundary conditions at the domain inlet and outlet respectively, since to fix the mass flow rate did not physically create the right condition. In 2002, a further step forward in the successful application of the Computational Fluid Dynamics (CFD) to studies on unsteady phenomena was made by Sano et al. [39] who numerically analysed the development of the flow instabilities in a vaned diffuser. This numerical analysis properly reproduced the RSI in a pump and the consequent development of the rotating stall, bringing about an exchange of flow direction in the diffuser channels in line with the results of the experimental analysis carried out on the same pump. Instantaneous pictures of two channels of the vaned diffuser at two different instants together with a flow visualization obtained by the

numerical analysis, highlighted a reverse flow from the diffuser discharge to the diffuser throat. Few moments later a jet flow appears in the channel and the reverse flow is moved to adjacent one (leakage flow). These flow patterns were also quite well captured by the numerical analysis. However, the adoption of a standard k-ε turbulence model still limited the capability of the numerical analysis of reproducing such unsteady phenomena: for example a different number of stall cells is determined.

For the first time, Pedersen et al. [40] experimentally captured instantaneous flow fields of two adjacent channels of a six-blade runner by using Particle Image Velocimetry (PIV). This analysis allowed to study the flow evolution in the runner at partial loads, highlighting an alternation of stalled and un-stalled passages. A stationary inlet stall cell blocks three-quarters of the entrance of one channel. The flow coming from the runner turned in the unstalled adjacent one. However, unlike the previous study, this did not evolve into a rotating stall, maybe because of the even number of passages, enabling a sort of equilibrium in the runner. A numerical analysis was also carried out by the same authors on the same six-bladed centrifugal pump, focusing on the appropriate choice of the turbulence model [41]. The comparison with the experimental results obtained by PIV analysis [40] allowed them to identify the LES (Large Eddy Simulation) model, adopted for the first time in that type of analysis, as more accurate in flow field prediction than the state-of-the-art turbulence models (k-ε and Baldwin-Lomax models), currently adopted in that period.

To identify the stator geometrical parameters mainly interacting with the flow at the runner exit, Hong and Kang [42] installed at the vaneless diffuser exit a fence, having a sinusoidal width variation (Z) as a function of the circumferential position (θ) (Figure 6). This fence created a blockage in the spanwise direction and mainly affected the radial velocity in comparison with the tangential velocity. This influence strongly varied according to the considered circumferential position, due to the sinusoidal variation of the fence width, causing a circumferential distortion of the flow field. Majidi [43] detected a similar unsteady circumferential distortion resulting from the RSI and went on to further investigate its influence on the mass distribution among the runner passages and on the blade loads, whose fluctuations were significantly amplified at part loads.
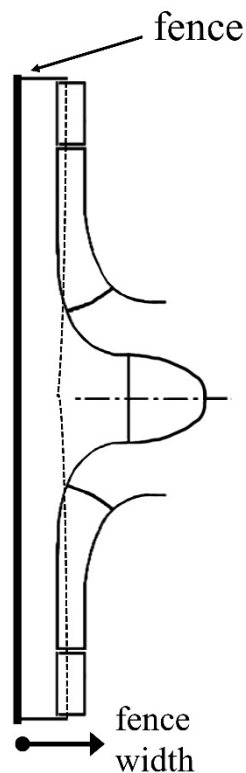
Figure 6 Schematic reconstruction of the analysed configuration with details of the fence positioned at the runner exit

The danger related to the possible onset of dynamic effects due to the RSI brought the scientific community to pay attention to the frequencies related to these pressure fluctuations [44]. These frequencies could coincide with the natural frequencies of the machine, causing the onset of dangerous resonance phenomena. Within this framework, Rodriguez et al. [45] proposed a theoretic model to estimate the frequencies related to the RSI. However, a single practical case was presented to verify their method, which resulted in a partial validation. Pavesi et al. [46] then went on with the investigation on RSI frequency content, by applying for the first time the wavelet analysis on unsteady pressure signals to characterize the onset and development of flow unsteadiness both in frequency and in time. Consequently, they revealed a rotating structure of pressure pulsations at the runner exit, appearing and disappearing in time with increasing intensity at part loads. In multi-stage RPTs, this strong RSI increases its intensity in a specific range of flow rates (0.60-0.90 of the design flow rate) [47].

Even though the hump zone, through a number of experimental analyses, was correlated with the RSI [48], the understanding of the related instability was significantly boosted by CFD (Computational Fluid Dynamics). Thanks to CFD and to the huge improvement in processor speed and counts, the flow field evolution in the whole pump was analysed in detail. A simulation carried out in the hump zone on an entire stage of a multi-stage RPT, leakage system included, was proposed by Cavazzini et al. [49]. Because of the revealed loss of accuracy of the LES model in the flow region close to the walls, they decided to adopt the DES model (Detached Eddy Simulation) which switches the turbulence treatment from the LES to the RANS (Reynolds-Averaged Navier Stokes) model in the near-wall regions. Thanks to this approach, they identified stall cells not only in the runner but also in the stator channels (Figure 7). Reverse flow cells arose on the runner blade

suction sides and moved downstream along the blade length (see for example the evolution of the reverse flow cell in passage A in Figure 7). The vaned diffuser passages were affected by unsteady perturbations, partly or totally obstructing the channel throat (see for example between diffuser blades 8 and 9 at instant t_3 in Figure 7). These unsteady perturbations forced the flow to the adjacent diffuser passage (see for example between diffuser blades 9 and 10 at instant t_3 in Figure 7) with the consequent onset of unsteady flow jets. These unsteady perturbations seemed to be related to vortexes developing downstream in the first portion of the return channel and partially (see Figure 8a) or totally (see Figure 8b) blocking the flow coming out from the diffuser. This strong rotor-stator interaction leaded not only to asymmetrical characteristics of the flow discharged by the runner but also to intense pressure pulsations at part loads and particularly in the hump zone.
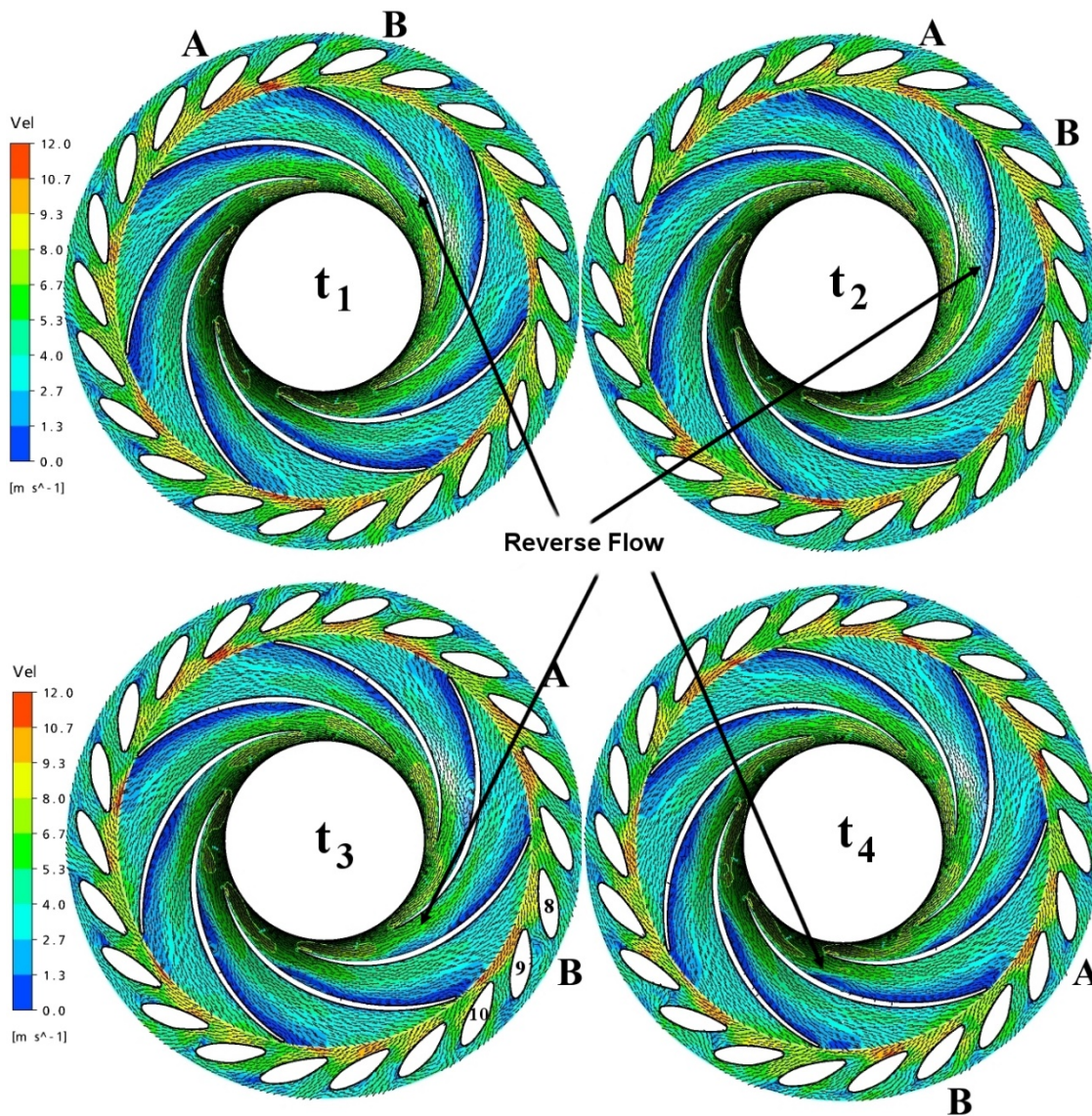

Figure 7 Flow field in the runner and diffuser at mid-span (Q/Q_{des}= 50%) at four time instants (Δt=47°)
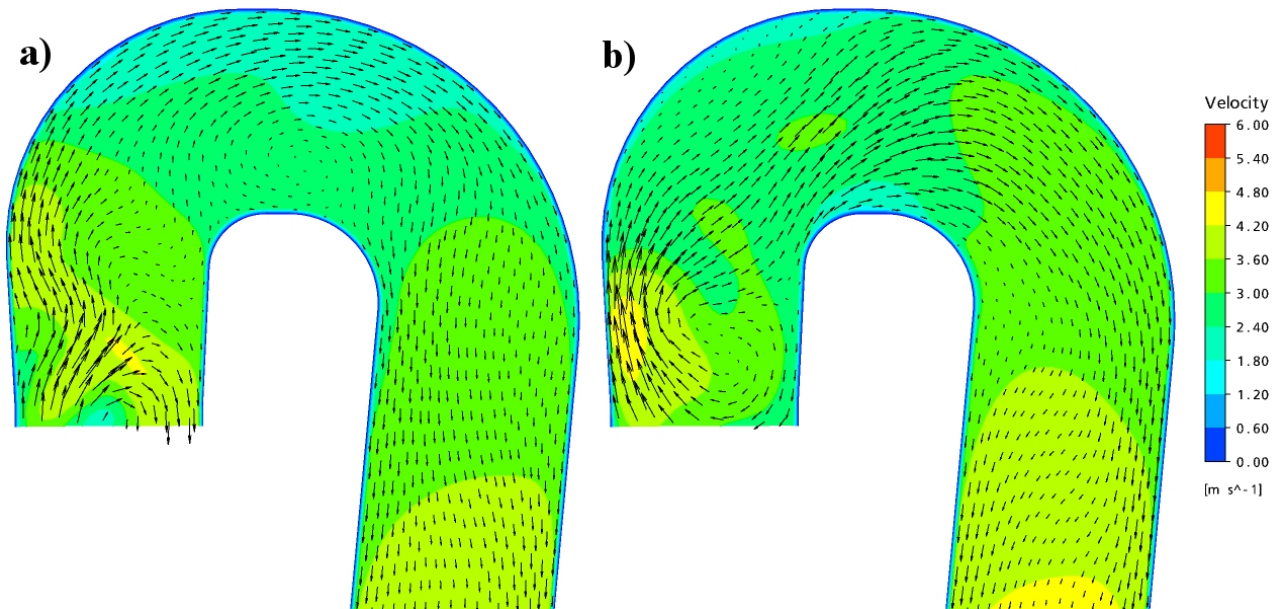
Figure 8 Vortexes developing in meridional sections of the first part of the return channel for Q/Q$_{des}$=50% partially (a) and totally (b) blocking the flow coming out from the diffuser

The interaction between a stall phenomenon in the stator and reverse flow cells on the blade suction of the runner was also confirmed by Jintao et al. [50] who tried to improve the numerical analysis of the flow field in the hump zone by adopting a two-phase model to take into account the cavitation incipience at the runner inlet. Unsteady numerical analyses in a RPT allowed Gentner et al. [51] to highlight the dependence of the unstable phenomena on the RPT specific speed. In particular, the hump zone of RTP characterized by high specific speed values (i.e. low head reversible pump turbine design), was linked to a vortex area, located in the runner close to the shroud and spreading from the runner inlet beyond the leading edge of the runner blade. In this case, no contribution to the head drop was provided by the rotating stall in the stator, which is identifiable even in stable operating conditions (i.e. outside the hump zone). A different behaviour was found for RTPs having low values of the specific speed (i.e. high head reversible pump turbine design). In this case, the hump zone in the head-discharge curve was linked to the strong interaction between the recirculation area, identified for high-specific speed RTPs, and a stall evolving in the stator (Figure 9), confirming the flow field evolution identified by Cavazzini et al. [49].
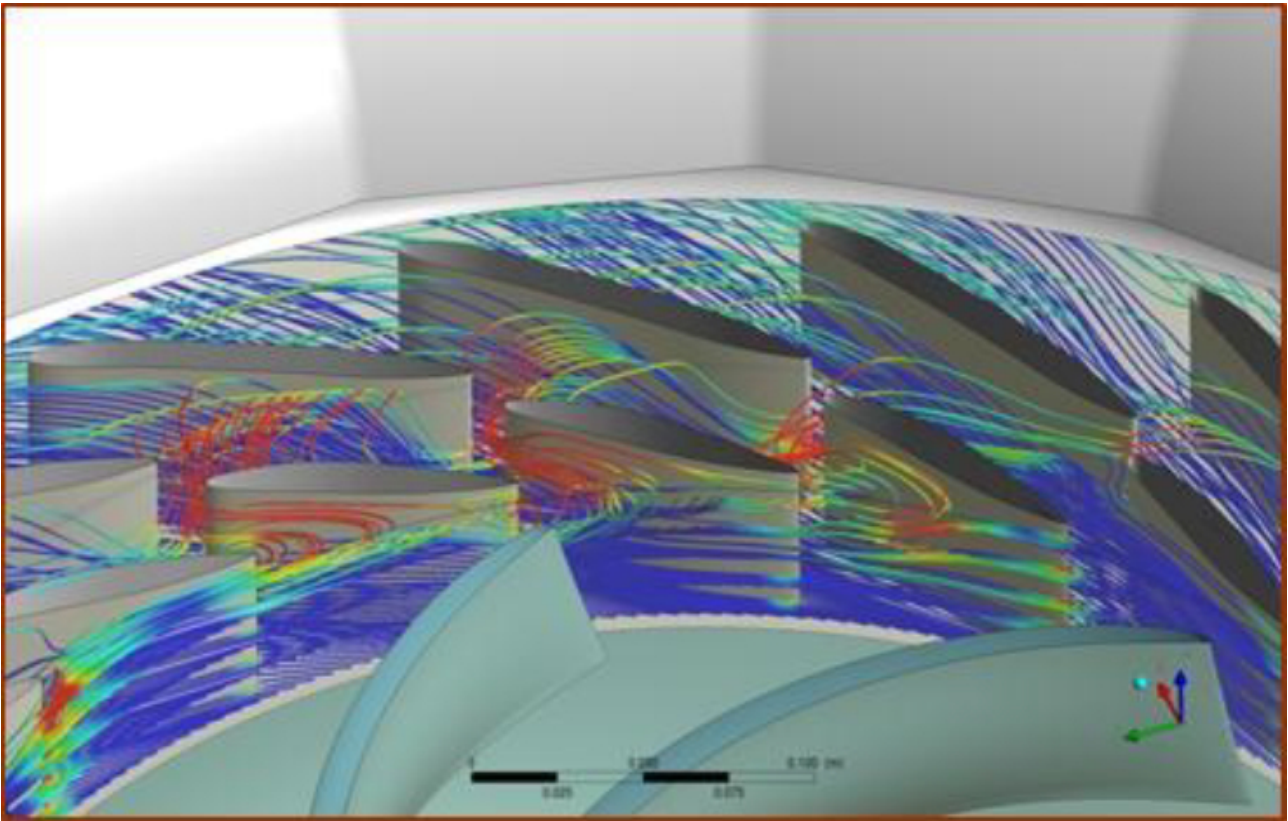
Figure 9 Stall cells in the stator for an unstable operating point in the hump zone [51]

Low specific speed RPTs were also experimentally investigated by Yang et al. [52] who identified the development in the stator parts of two phenomena, spectrally identified with two fundamental frequencies. The first of these phenomena due to vortexes in the return channel was not significant for the hump zone since it resulted to develop even in stable operating conditions. However, this phenomenon was demonstrated to interact with a second unsteady three-dimensional flow structure developing into the diffuser vane channels in the hump region.

Even though the combination between experimental analyses and CFD has made it possible to characterize the pump-turbine unstable operating range in pumping mode and to study in depth its fluid-dynamical development [53], to the authors' knowledge no one has identified the dependency between the RPT design and the onset of this unstable behavior. Today, there is no identified innovative design criteria aimed at eliminating or, at least, moving out of the normal and continuous operating range this hump zone.

4. Instability in turbine mode: the S-Shape zone

The design of a RPT represents a compromise among several design needs, requesting different design strategies depending on the considered machine operating mode (pump or turbine mode). The design criterion mainly adopted focuses on the pump performance, greatly affected by flow separations and instabilities. However, this design criterion may give rise to instability behaviour in turbine mode, that is the typical S-Shaped profile in the Q_{11}-n_{11} characteristic curve (Figure 3) [54]. If this S-Shaped profile is near the runaway

condition, the RPT may alternate between generating and reverse pumping mode only for a rotational speed variation of 2 rpm [54]. If no specific control solutions are put in place, such as adequate closing laws for main inlet valve and/or for guide vanes, the resulting transient behavior may cause not only high levels of torque fluctuations but also marked variations of the discharge rate and head. This behavior may cause water hammers and strong resonant vibrations [51], [55] with consequent damages for the mechanical equipment but also for the entire PHES [16], [29], [30].

4.1 Characterization of the S-Shape phenomena

Recently, several authors have tried to identify and characterize the phenomena causing the S-Shaped characteristic by means of in-depth studies of the RPT unstable operating area. In 2011, Hasmatuchi et al. [56], [57] analyzed the fluid flow in a high head reversible pump turbine at different operating points from the best efficiency condition to the turbine brake area. In the unstable operating range, they identified the onset of a rotating stall in the rotor-stator radial gap with a frequency equal to 70% of the RPT rotation rate. Intense flow detachments from the runner blades block some of the runner channels and, at very low positive discharge flow rates, induce reverse flows and vortexes in the guide vanes, causing the onset of a stall cell. Pressure pulsations in the wicket gates and downstream resulted to be 25 times greater than those at design operating conditions if accompanied by the rotating stall [58]. Seidel et al. [59] numerically analysed a load rejection scenario, numerically bringing the RTP, entirely modeled, from the stable operating point to the brake area at constant guide vane opening. Their analysis confirmed the onset of flow instabilities in the runner at runaway conditions, whose intensity increased in the S-Shape region, evolving in a stall cell rotating at a sub synchronous frequency of the runner rotational speed and blocking the flow in some runner channels. At lower discharge conditions, the stall was so large to affect not only the runner flow field but also the flow in the rotor-stator gap and in the channels of stay and guide vanes, thus supporting the hypothesis of Hasmatuchi et al. [57]. A total pressure rise over the machine accompanied the development of a recirculating flow region caused by the rotating stall.

A step forward in the understanding of the phenomena related to the S-Shape profile was made by Gentner et al. [51] who simulated the evolution in time of the flow field during the turbine brake of pump-turbines with and without the S-Shape characteristic. Their analysis highlighted, in both cases, the development of a complex structure, composed by two vortexes, a primary one in the rotor-stator gap combined with a secondary one evolving in the runner channels. For the RPT without S-Shape characteristic, the blockage action of the vortex structure is only partial and the fluid flows into the runner channels near hub and shroud. For the RPT with S-Shape, the vortex structure increased its extension, blocking the inlet area of the runner channels with a significant pressure increase in the spiral casing. No specific frequency was associated to this vortex structure in the S-Shape area [60]. Widmer et al. [61] went on with the investigation of the time-varying flow field evolution in the S-Shape region and numerically reproduced two different scenarios:

1. A load rejection scenario characterized by a progressive reduction of the flow rate up to the turbine brake area at constant guide vane angle. Different wicket gate angles were considered in order to investigate their influence on the flow characteristics

2. A starting scenario characterized by a progressive increase of the flow rate and of the guide vane opening angle starting from an unstable operating condition in the S-Shape region.

Both these cases confirmed the development of unsteady vortexes, evolving into a rotating stall, in the rotor and stator channels at large guide vane angles. At smaller angles this unsteady behaviour did not arise because of the increase in the rotor-stator radial gap. In this study, the analyses also highlighted the development of vortexes circumferentially distributed around the whole runner entrance.

The load rejection scenario of a low-specific speed RPT (constant guide vane angle) was also numerically analysed by Cavazzini et al. [62]. They identified a partial or complete blockage action made by stall cells in rotor and stator passages, causing increasing fluctuations of the discharge rate in the passages, of the pressure distributions and torque exerted on the blades. Via wavelet analysis of the numerical signals, they also showed that blocking vortexes in the RTP are not sufficient for generating the S-Shape in the Q_{11}-n_{11} curve. The increase in head, at the basis of the S-Shape feature, started only when these vortexes evolved in a more organized structure, rotating with a specific frequency (i.e. rotating stall). Starting from this correlation between S-Shape in RTP curves and rotating stall, Botero et al. [63] proposed a method for predicting the rotating stall onset, based on the analysis frequencies of the wicket gates vibrations.

4.2 Innovative design criteria

To date, the authors believe that the root causes of the turbine unstable behaviour are still not completely identified and, as a consequence, the definition of innovative design criteria still represents a challenge. Nonetheless, some geometry modifications aimed at improving the RPT's stability were proposed in literature. Gentner et al. [51] focused on the leading edge of the blade runner, demonstrating a correlation with the S-Shape in turbine mode and proposed new runner models to avoid fully-developed vortexes near the runaway condition. Experimental analyses demonstrated the effectiveness of these modifications in eliminating the S-Shape for the relevant guide vane angles, but also highlighted a corresponding reduction of the runner efficiency in pump operation. Unfortunately, no details about geometry modifications and their effects on the flow field in pumping mode were presented. Olimstad et al. [64] observed a correlation between S-Shape and the RPT design criteria, by comparing the flow field of the RPT with that of a typical Francis turbine at the same operating conditions. Different geometrical configurations, characterized by changes in the runner geometry small enough not to affect the performance at the design operating condition were tested. In turbine mode at part load, the machine's behaviour resulted to be positively affected by an increase of the blade length and of the angle and of the radius of the leading edge on the pressure side. Positive results were also achieved by a reduction of the inlet radius.

Starting from the original RPT design, Houdeline et al. [19] attempted to positively affect the RPT behavior in the unstable areas by geometry modifications. Since they did not intend to alter the main performance in pumping mode, they did not significantly change the main runner dimensions and the high-pressure diameter, but only secondary design parameters, obtaining significant improvements of the S-Shape characteristics. Yin et al. [65] focused on the runner design and obtained an improvement of the S-Shape characteristic by broadening the meridional section of the runner. However, this modification also significantly affected the

machine's performance in pumping mode with a remarkable increase of the head, especially at larger flow rates.

4.3 Effects of the misaligned guide vanes (MGV) technique on pump-turbine stability in generation mode

In 1982 Klemm [66] set out to improve the RTP stable behavior, proposing the technique of the "misaligned guide vanes" (MGV), consisting in changing the opening of an even number of guide vanes to proper pre-opening angles (Figure 10).
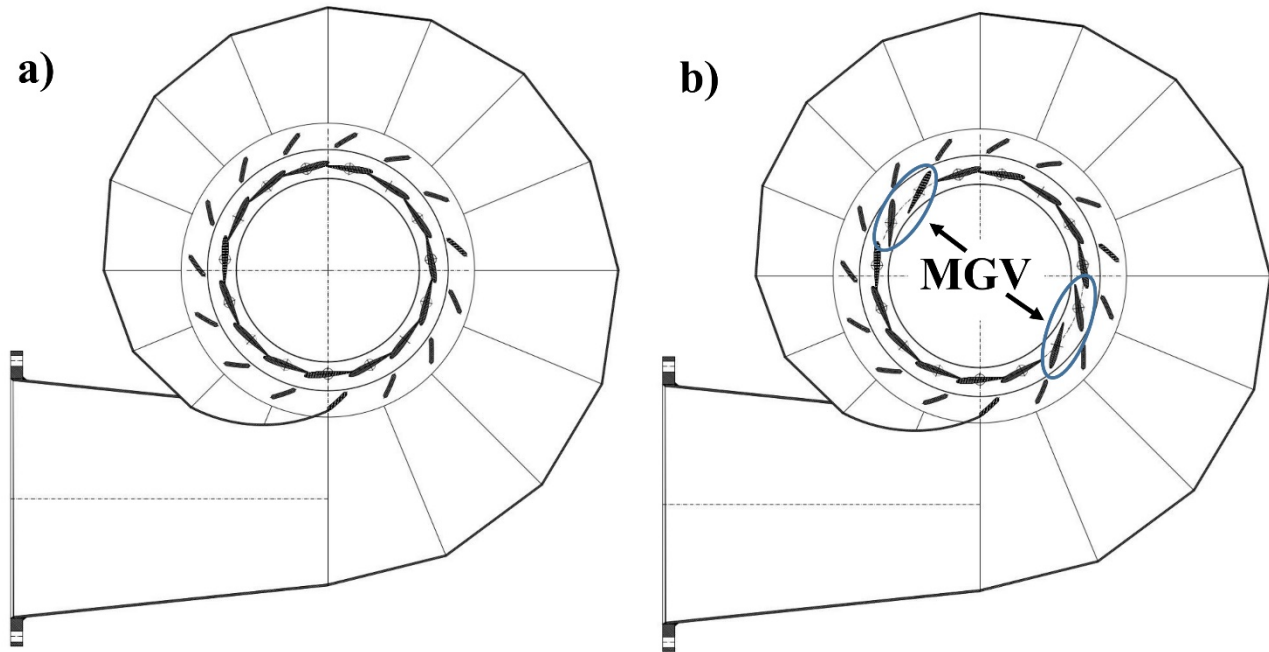

Figure 10 Scheme of the misaligned guide vanes technique: a) synchronous guide vanes b) misaligned guide vanes

The effectiveness of this technique during the turbine start-up, during load rejection and in no-load condition was demonstrated by Shao [67], who established the medication of the RPT characteristics by adoption of the MGVs technique, starting from those without MGVs. However, although adopting such a technique the blockage due to the rotating stall was reduced and the S-Shaped characteristic eliminated, pressure fluctuations and unbalanced radial forces on the runner resulted to increase, with a consequent unstable behavior at no-load condition, as demonstrated by Sun et al [68] in 2013. Xiao et al. [69] numerically demonstrated that this increase in pressure fluctuations and radial forces is related to the destruction of the fluid-dynamical axial-symmetry in the guide-vanes and runner blade passages.

5. Conclusions

The deployment of the huge potential of intermittent and unpredictable renewable energy sources is significantly limited by their negative impact on safety, stability and efficiency of the electricity grid. To mitigate these impacts allowing for an increase in green energy production, PHES are required to overcome

their instability limits so as to significantly wide their operating range and to further develop their frequency regulation services (fast response time, extended power range, operation at part-loads,…). In such a context, there is an urgent need to develop a new concept of pump-turbine, whose design has to be built on an in-depth knowledge and a complete understanding of the instabilities affecting the pump-turbine behavior.

The paper presents an in-depth description of the possible operating modes encountered by a RPT in a PHES, highlighting the effects of the development of unstable phenomena inside the machine on the global plant behaviour. It clarifies why the normal and continuous operating range of a RPT is affected and limited by its stable or unstable hydraulic characteristics and how this reflects on the plant capability to start-up, shut-down or change its operating mode in order not only to provide regulation but also to face normal or emergency situations (load rejection, power failure, etc…).

To clarify the reasons of this unstable behaviour, a detailed review of the studies published in literature on the unsteady phenomena developing in pumping and generating modes, with a particular focus on the most significant results achieved and on the adopted approaches, has been presented.

As regards pump mode, the unstable operating area, identified by the hump zone (positive slope of the head-discharge curve), was closely linked to the inception of different types of rotating stalls or structures of pressure pulsations due to rotor-stator interaction mechanisms. These unsteady phenomena cause an amplification of the runner and stator hydraulic losses, resulting in a drop of the RPT head and in strong vibrations on the mechanical components. Even though the combination between experimental analyses and CFD has made it possible to study in depth their fluid-dynamical development, only a relation between this unstable behaviour and the rotor-stator radial gap and the RPT specific speed has been argued. Today, to the authors' knowledge there is no identified innovative design criteria aimed at eliminating or, at least, reducing the limits imposed by this hump zone on the normal and continuous operating range.

As regards the turbine mode, the unstable behavior, associated with the increase in head at part loads (negative slope in the head-discharge curve), was related to the blocking action of vortexes and/or stall cells, imposing a pumping behavior to some runner blades. For the RPTs affected by the S-shape behavior, normal small speed variations (ex. 2 rpm) would determine a sudden change of operating mode, forcing the RTP to continuously switch to and for from pump to turbine mode. Specific control solutions such as adequate closing laws for the main inlet valve and/or for guide vanes have to be put in place to avoid risks of damage to electrical and mechanical equipment of the power plant. However, these solutions are able to control but not to eliminate the critical transient behaviour during turbine stops or synchronization. Some geometrical parameters positively affecting the flow mechanisms developing in S-Shape regions have been identified (shape of the blade's leading edge, inlet blade angle, blade length, etc..). However, modifications in these parameters resulted to have negative impact on the RPT's performance in pumping mode.

So, it is in the authors' opinion that the only way to successfully overcome the stability problems of RPT is to consider simultaneously the complexity of the phenomena in both the operating modes (generating and pumping mode). This approach will require to take into account a huge number of design parameters and this will be possible only by adopting new design approaches, based on advanced multi-objective optimization

methods combined with CFD. These methods would allow simultaneously taking into account the opposing targets of a RPT design in order to define innovative design criteria, representing the best compromise between performance, stable behavior and regulation capacity in both operating modes.

Acknowledgements

References

[1]   ENTSO (European Transmission System Operators), *Towards A Successful Integration of Large Scale Wind Power into European Electricity Grids. Final Report.* European Wind Integration Study (EWIS), 2010.

[2]   J. P. S. Catalão, *Smart and sustainable power systems : operations, planning, and economics of insular electricity grids*. .

[3]   J. S. Anagnostopoulos and D. E. Papantonis, "Study of pumped storage schemes to support high RES penetration in the electric power system of Greece," *Energy*, vol. 45, no. 1, pp. 416–423, 2012.

[4]   B. Steffen, "Prospects for pumped-hydro storage in Germany," *Energy Policy*, vol. 45, pp. 420–429, 2012.

[5]   M. Aneke and M. Wang, "Energy storage technologies and real life applications – A state of the art review," *Appl. Energy*, vol. 179, pp. 350–377, Oct. 2016.

[6]   N. S. Pearre and L. G. Swan, "Technoeconomic feasibility of grid storage: Mapping electrical services and energy storage technologies," *Appl. Energy*, vol. 137, pp. 501–510, Jan. 2015.

[7]   K. Bradbury, L. Pratson, and D. Patiño-Echeverri, "Economic viability of energy storage systems based on price arbitrage potential in real-time U.S. electricity markets," *Appl. Energy*, vol. 114, pp. 512–519, Feb. 2014.

[8]   J. P. Deane, B. P. O Gallachoir, and E. J. McKeogh, "Techno-economic review of existing and new pumped hydro energy storage plant," *Renew. Sustain. Energy Rev.*, vol. 14, no. 4, pp. 1293–1302, 2010.

[9]   D. M. Greenwood, K. Y. Lim, C. Patsios, P. F. Lyons, Y. S. Lim, and P. C. Taylor, "Frequency response services designed for energy storage," *Appl. Energy*, vol. 203, pp. 115–127, Oct. 2017.

[10]   T. Kunz, A. Schwery, and G. Sari, "Adjustable speed pumped storage plants - innovation challenges and feedback of experience from recent projects," in *17th International Seminar on Hydropower Plants: pumped storage in the context of renewable energy supply*, 2012, pp. 245–260.

[11] G. D. Ciocan, O. Teller, and F. Czerwinski, "Variable Speed Pump-Turbines Technology," *U.P.B. Sci. Bull.*, vol. 74, no. 1, pp. 33–42, 2012.

[12] J. M. Henry, J.-B. Houdeline, S. Ruiz, and T. Kunz, "How reversible pump-turbines can support grid variability: The variable speed approach," *Int. J. Hydropower Dams*, vol. 20, no. 5, pp. 68–73, 2013.

[13] R. S. Stelzer and R. N. Walters, "Estimating Reversible Pump-Turbine Characteristics," *Engineering*, no. 39, pp. 1–39, 1977.

[14] J.-I. Perez-Diaz, G. Cavazzini, F. Blazquez, C. Platero, J. Fraile-Ardanuy, J. A. Sanchez, and M. Chazarra, "Technological developments for pumped-hydro energy storage," Bruxelles, 2014.

[15] D. Beevers, L. Branchini, V. Orlandini, A. De Pascale, and H. Perez-Blanco, "Pumped hydro storage plants with improved operational flexibility using constant speed Francis runners," *Appl. Energy*, vol. 137, pp. 629–637, Jan. 2015.

[16] S. Pejovic, Q. F. Zhang, B. Karney, and A. Gajic, "Analysis of Pump-Turbine ' S ' Instability and Reverse Waterhammer Incidents in Hydropower Systems," in *4-th International Meeting on Cavitation and Dynamic Problems in Hydraulic Machinery and Systems*, 2011.

[17] A. Rezghi and A. Riasi, "The interaction effect of hydraulic transient conditions of two parallel pump-turbine units in a pumped-storage power plant with considering 'S-shaped' instability region: Numerical Simulation," *Renew. Energy*, vol. 118, pp. 896–908, 2018.

[18] G. Ardizzon, G. Cavazzini, and G. Pavesi, "A new generation of small hydro and pumped-hydro power plants: Advances and future challenges," *Renew. Sustain. Energy Rev.*, vol. 31, pp. 746–761, 2014.

[19] J.-B. Houdeline, J. Liu, S. Lavigne, Y. Laurant, and L. Balara, "Start-up improvement in turbine mode for high head PSP machine," *IOP Conf. Ser. Earth Environ. Sci.*, vol. 15, p. 42022, 2012.

[20] International Electrotechnical Commission, *IEC 60193 - Hydraulic turbines, storage pumps and pump-turbines – Model acceptance tests*, 2nd ed., vol. 60193. International Electrotechnical Commission, 1999.

[21] D. Li, H. Wang, Z. Li, T. K. Nielsen, X. Wei, and D. Qin, "Transient characteristics during the closure of guide vanes in a pump- turbine in pump mode," *Renew. Energy*, vol. 118, pp. 973–983, 2018.

[22] E. Egusquiza, C. Valero, D. Valentin, A. Presas, and C. G. Rodriguez, "Condition monitoring of pump-turbines. New challenges," *Meas. J. Int. Meas. Confed.*, vol. 67, pp. 151–163, 2015.

[23] P.-Y. Lowys, F. Andre, A. Ferreira da Silva, F. Duarte, and J.-P. Payre, "Hydro Plant Operating Range Extension - Transverse Approach for Increasing Turbine Flexibility," in *Hydrovision International 2014*, 2014.

[24] C. Trivedi, E. Agnalt, and O. G. Dahlhaug, "Investigations of unsteady pressure loading in a Francis turbine during variable-speed operation," *Renew. Energy*, vol. 113, pp. 397–410, 2017.

[25] C. Trivedi, E. Agnalt, and O. G. Dahlhaug, "Experimental study of a Francis turbine under variable-speed and discharge conditions," *Renew. Energy*, vol. 119, pp. 447–458, 2018.

[26] H. Zhang, D. Chen, C. Wu, X. Wang, J. M. Lee, and K. H. Jung, "Dynamic modeling and dynamical analysis of pump-turbines in S-shaped regions during runaway operation," *Energy Convers. Manag.*, vol. 138, pp. 375–382, 2017.

[27] W. Zeng, J. Yang, J. Hu, and J. Yang, "Guide-Vane Closing Schemes for Pump-Turbines Based on Transient Characteristics in S-shaped Region," *J. Fluids Eng.*, vol. 138, no. 5, p. 051302, 2016.

[28] R. Goyal and B. K. Gandhi, "Review of hydrodynamics instabilities in Francis turbine during off-design and transient operations," *Renew. Energy*, vol. 116, pp. 697–709, 2018.

[29] B. Karney, A. Gajic, and S. Pejovic, "Case studies - Our experience in hydraulic transients and vibrations," in *Proceedings of the International Conference on CSHS03*, 2003, pp. 1–17.

[30] S. Pejovic, L. Krsmanovic, R. Jemcov, and P. Crnkovic, "Unstable Operation of High-Head Reversible Pump-Turbines," in *Proc. of 8th IAHR Symp. on Hydr. Mach. and Cavitation*, 1976, pp. 283–295.

[31] N. Arndt, A. J. Acosta, C. E. Brennen, and T. K. Caughey, "Rotor-Stator Interaction in a Diffuser Pump," *J. Turbomach.*, vol. 111, pp. 213–221, 1989.

[32] N. Arndt, A. J. Acosta, C. E. Brennen, and T. K. Caughey, "Experimental Investigation of Rotor-Stator Interaction in a Centrifugal Pump With Several Vaned Diffusers," *J. Turbomach.*, vol. 112, pp. 98–108, 1990.

[33] R. Dong, S. Chu, and J. Katz, "Quantitative visualization of the flow within the volute of a centrifugal pump. Part B: results and analysis," *J. Fluids Eng. Trans. ASME1*, vol. 114, pp. 396–403, 1992.

[34] O. Akin and D. Rockwell, "Flow structure in a Radial Flow Pumping System Using High-Image-Density Particle Image Velocimetry," *J. Fluids Eng. Trans. ASME*, vol. 116, pp. 538–544, 1994.

[35] O. Akin and D. Rockwell, "Interaction of zones of flow separation in a centrifugal impeller-stationary vane system," *Exp. Fluids*, vol. 17, no. 6, pp. 427–433, 1994.

[36] M. Sinha, A. Pinarbasi, and J. Katz, "The Flow Structure During Onset and Developed States of Rotating Stall Within a Vaned Diffuser of a Centrifugal Pump," *J. Fluids Eng.*, vol. 123, no. 3, p. 490, 2001.

[37] T. Sano, Y. Nakamura, Y. Yoshida, and Y. Tsujimoto, "Alternate Blade Stall and Rotating Stall in a Vaned Diffuser," *JSME Int. J. - Ser. B*, vol. 45, no. 4, pp. 810–819, 2002.

[38] J. González, J. Fernández, E. Blanco, and C. Santolaria, "Numerical Simulation of the Dynamic Effects Due to Impeller-Volute Interaction in a Centrifugal Pump," *J. Fluids Eng.*, vol. 124, no. 2, p. 348, 2002.

[39] T. Sano, Y. Yoshida, Y. Tsujimoto, Y. Nakamura, and T. Matsushima, "Numerical Study of Rotating Stall in a Pump Vaned Diffuser," *J. Fluids Eng.*, vol. 124, no. 2, p. 363, 2002.

[40] N. Pedersen, P. S. Larsen, and C. B. Jacobsen, "Flow in a Centrifugal Pump Impeller at Design and Off-Design Conditions—Part I: Particle Image Velocimetry (PIV) and Laser Doppler Velocimetry (LDV) Measurements," *J. Fluids Eng.*, vol. 125, no. 1, p. 61, 2003.

[41] R. K. Byskov, C. B. Jacobsen, and N. Pedersen, "Flow in a Centrifugal Pump Impeller at Design and

Off-Design Conditions—Part II: Large Eddy Simulations," *J. Fluids Eng.*, vol. 125, no. 1, p. 73, 2003.

[42] S.-S. Hong and S.-H. Kang, "Flow at the Centrifugal Pump Impeller Exit With Circumferential Distortion of the Outlet Static Pressure," *J. Fluids Eng.*, vol. 126, no. 1, p. 81, 2004.

[43] K. Majidi, "Numerical Study of Unsteady Flow in a Centrifugal Pump," *J. Turbomach.*, vol. 127, no. 2, p. 363, 2005.

[44] S. Guo and Y. Maruta, "Experimental Investigations on Pressure Fluctuations and Vibration of the Impeller in a Centrifugal Pump with Vaned Diffusers," *JSME Int. J. Ser. B*, vol. 48, no. 1, pp. 136–143, 2005.

[45] C. G. Rodriguez, E. Egusquiza, and I. F. Santos, "Frequencies in the Vibration Induced by the Rotor Stator Interaction in a Centrifugal Pump Turbine," *J. Fluids Eng.*, vol. 129, no. 11, p. 1428, 2007.

[46] G. Pavesi, G. Cavazzini, and G. Ardizzon, "Time-frequency characterization of the unsteady phenomena in a centrifugal pump," *Int. J. Heat Fluid Flow*, vol. 29, no. 5, pp. 1527–1540, 2008.

[47] J. F. Gülich, *Centrifugal pumps*. New York: Springer Berlin Heidelberg, 2010.

[48] G. Lu, Z. Zuo, Y. Sun, D. Liu, Y. Tsujimoto, and S. Liu, "Experimental evidence of cavitation influences on the positive slope on the pump performance curve of a low specific speed model pump-turbine," *Renew. Energy*, vol. 113, pp. 1539–1550, 2017.

[49] G. Cavazzini, G. Pavesi, and G. Ardizzon, "Pressure instabilities in a vaned centrifugal pump," *Proc. Inst. Mech. Eng. Part A J. Power Energy*, vol. 225, no. 7, pp. 930–939, 2011.

[50] J. Liu, S. Liu, Y. Wu, L. Jiao, L. Wang, and Y. Sun, "Numerical investigation of the hump characteristic of a pump-turbine based on an improved cavitation model," *Comput. Fluids*, vol. 68, pp. 105–111, 2012.

[51] C. Gentner, M. Sallaberger, C. Widmer, and O. Braun, "Analysis of unstable operation of pump turbines and how to avoid it," in *Hydro -Innovative Approaches to Global Challenges*, 2012, pp. 1–8.

[52] J. Yang, G. Pavesi, S. Yuan, G. Cavazzini, and G. Ardizzon, "Experimental characterization of a pump-turbine in pump mode at hump instability region," *J. Fluids Eng. Trans. ASME*, vol. 137, no. 5, 2015.

[53] D. Li, H. Wang, Y. Qin, X. Wei, and D. Qin, "Numerical simulation of hysteresis characteristic in the hump region of a pump-turbine model," *Renew. Energy*, vol. 115, pp. 433–447, 2018.

[54] G. Olimstad, T. Nielsen, and B. Børresen, "Stability Limits of Reversible-Pump Turbines in Turbine Mode of Operation and Measurements of Unstable Characteristics," *J. Fluids Eng. - Trans. ASME*, vol. 134, no. 11, p. 111202, 2012.

[55] J. X. Zhou, B. W. Karney, M. Hu, and J. C. Xu, "Analytical study on possible self-excited oscillation in S-shaped regions of pump-turbines," in *Proceedings of the Institution of Mechanical Engineers, Part A: Journal of Power and Energy*, 2011, vol. 225, no. 8, pp. 1132–1142.

[56] V. Hasmatuchi, "Hydrodynamics of a Pump-Turbine Operating at Off-Design Conditions in Generating Mode," École Polytechnique Fédérale de Lausanne, 2012.

[57] V. Hasmatuchi, M. Farhat, S. Roth, F. Botero, and F. Avellan, "Experimental Evidence of Rotating Stall in a Pump-Turbine at Off-Design Conditions in Generating Mode," *J. Fluids Eng.*, vol. 133, no. 5, p. 051104, 2011.

[58] V. Hasmatuchi, "Experimental Investigation of a pump-turbine at off-design operating conditions," *3rd IAHR Int. Meet. Workgr. Cavitation Dyn. Probl. Hydraul. Mach. Syst. Oct. 14-16, 2009, Brno, Czech Repub.*, vol. 3, pp. 339–348, 2009.

[59] U. Seidel, J. Koutnik, and M. Giese, "S-curve characteristics of pump-turbines," in *Hydro -Innovative Approaches to Global Challenges*, 2012, pp. 1–9.

[60] C. Gentner, M. Sallaberger, C. Widmer, B.-J. Bobach, H. Jaberg, J. Schiffer, and M. Guggenberger, "Comprehensive experimental and numerical analysis of instability phenomena in pump turbines," in *IOP Conference Series: Earth and Environmental Science*, 2014, vol. 22, p. 032046.

[61] C. Widmer, T. Staubli, and N. Ledergerber, "Unstable Characteristics and Rotating Stall in Turbine Brake Operation of Pump-Turbines," *J. Fluids Eng.*, vol. 133, no. 4, p. 041101, 2011.

[62] G. Cavazzini, A. Covi, G. Pavesi, and G. Ardizzon, "Analysis of the Unstable Behavior of a Pump-Turbine in Turbine Mode: Fluid-Dynamical and Spectral Characterization of the S-shape Characteristic," *J. Fluids Eng.*, vol. 138, no. 2, p. 021105, 2016.

[63] F. Botero, V. Hasmatuchi, S. Roth, and M. Farhat, "Non-intrusive detection of rotating stall in pump-turbines," *Mech. Syst. Signal Process.*, vol. 48, no. 1–2, pp. 162–173, 2014.

[64] G. Olimstad, T. Nielsen, and B. Børresen, "Dependency on Runner Geometry for Reversible-Pump Turbine Characteristics in Turbine Mode of Operation," *J. Fluids Eng.*, vol. 134, no. 12, p. 121102, 2012.

[65] J. Yin, D. Wang, X. Wei, and L. Wang, "Hydraulic Improvement to Eliminate S-Shaped Curve in Pump Turbine," *J. Fluids Eng.*, vol. 135, no. 7, p. 071105, 2013.

[66] D. Klemm, "Stabilizing the characteristics of a pump turbine in the range between turbine part load and reverse pump operation," *Voith - Forsch. und Konstr.*, vol. 82, 1982.

[67] W. Y. Shao, "Improving stability by misaligned guide ganes in pumped storage plant," *Asia-Pacific Power Energy Eng. Conf. APPEEC*, 2009.

[68] H. Sun, R.-F. Xiao, W. Liu, and F. Wang, "Analysis of S Characteristics and Pressure Pulsations in a Pump-Turbine With Misaligned Guide Vanes.," *J. Fluids Eng.*, vol. 135, no. 5, pp. 511011–511016, 2013.

[69] Y.-X. Xiao and R.-F. Xiao, "Transient simulation of a pump-turbine with misaligned guide vanes during turbine model start-up," vol. 30, pp. 646–655, 2014.